

Stabilization of mixed-phase structures in highly strained BiFeO₃ thin films via chemical-alloying

Anoop R. Damodaran, Eric Breckenfeld, Amber K. Choquette, and Lane W. Martin

Citation: *Appl. Phys. Lett.* **100**, 082904 (2012); doi: 10.1063/1.3688175

View online: <http://dx.doi.org/10.1063/1.3688175>

View Table of Contents: <http://apl.aip.org/resource/1/APPLAB/v100/i8>

Published by the [American Institute of Physics](http://www.aip.org).

Related Articles

Angular and frequency dependence of standing spin waves in FePt films

J. Appl. Phys. **111**, 033911 (2012)

Kinetics aspects of initial stage thin γ -Al₂O₃ film formation on single crystalline β -NiAl (110)

J. Appl. Phys. **111**, 034312 (2012)

Growth sector dependence and mechanism of stress formation in epitaxial diamond growth

Appl. Phys. Lett. **100**, 041906 (2012)

Role of atomic terraces and steps in the electron transport properties of epitaxial graphene grown on SiC

AIP Advances **2**, 012115 (2012)

Atomic configuration of the interface between epitaxial Gd doped HfO₂ high k thin films and Ge (001) substrates

J. Appl. Phys. **111**, 014102 (2012)

Additional information on *Appl. Phys. Lett.*

Journal Homepage: <http://apl.aip.org/>

Journal Information: http://apl.aip.org/about/about_the_journal

Top downloads: http://apl.aip.org/features/most_downloaded

Information for Authors: <http://apl.aip.org/authors>

ADVERTISEMENT



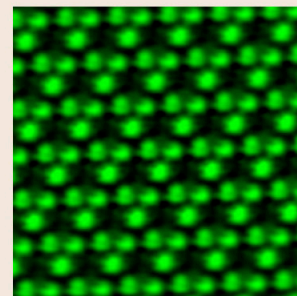
**ASYLUM
RESEARCH**
The Technology Leader in SPM/AFM

Register Now at
www.asylumresearch.com

Free AFM Webinar February 22 Register Now

“Smaller and Quieter: Ultra-High Resolution AFM Imaging”

With Jason Cleveland, AFM pioneer,
inventor and Asylum Research co-founder



Stabilization of mixed-phase structures in highly strained BiFeO₃ thin films via chemical-alloying

Anoop R. Damodaran, Eric Breckenfeld, Amber K. Choquette, and Lane W. Martin^{a)}

Department of Materials Science and Engineering and Materials Research Laboratory, University of Illinois, Urbana-Champaign, Urbana, Illinois 61801, USA

(Received 25 October 2011; accepted 4 February 2012; published online 22 February 2012)

Chemical-alloying is demonstrated to stabilize the mixed-phase structure of highly strained epitaxial BiFeO₃/LaAlO₃ (001) heterostructures. Such mixed-phase structures are essential for the large electromechanical responses (4%–5% strains under applied electric field); however, films with thickness exceeding 250 nm undergo an epitaxial breakdown to a non-epitaxial bulk-like rhombohedral-phase. Such an irreversible transformation of the mixed-phase structure limits the magnitude of the net surface displacement associated with these field-induced phase transformations. Using high-resolution x-ray diffraction reciprocal space mapping and scanning-probe-based studies, we show that chemical-alloying of BiFeO₃ thin films can stabilize these mixed-phase structures and delay the onset of epitaxial breakdown. © 2012 American Institute of Physics. [doi:10.1063/1.3688175]

BiFeO₃ is a room temperature multiferroic exhibiting antiferromagnetism that is coupled with ferroelectricity^{1,2} and is a candidate material for the replacement of lead-based ferroelectrics.^{3,4} In the recent years, it has been shown that thin films of BiFeO₃ under ~4.5% or more compressive strain undergo a strain-induced structural phase transition from a bulk-like rhombohedrally distorted perovskite structure (*R3c*) to a tetragonal-like phase (monoclinically distorted structure, derived from a *P4mm* parent-phase with *c/a* ~ 1.23).^{5–9} Moreover, as the thickness of the BiFeO₃/LaAlO₃ (001) heterostructure increases, the onset of complex mixed-phase structures in addition to the highly distorted, tetragonal-like phase has been observed. These mixed-phase structures consist of highly distorted and tilted monoclinic polymorphs of BiFeO₃ and are essential for the large electromechanical responses in this material.^{10,11} These mixed-phase films exhibit an enhanced piezoelectric coefficient ($d_{33} \sim 115$ pm/V) compared to the parent rhombohedral-like ($d_{33} \sim 53$ pm/V) and tetragonal-like ($d_{33} \sim 30$ pm/V) phases.^{10,12} The enhanced electromechanical response in these mixed-phase films has been attributed to the presence of complex structural phase boundaries present in these highly strained BiFeO₃ films and its ability to reversibly transform between structural polymorphs under applied electric field.^{11,13} The electric field modulated switching between the various polymorphs has been shown to be completely reversible and is accompanied by large surface displacements exceeding 4%–5% of the film thickness. Such observations have significant implications for applications in electromechanical devices including possibilities of ultra high-density probe-based data storage systems.^{13–15}

A breakdown in epitaxy and an irreversible transformation to a non-epitaxial bulk-like rhombohedral phase, however, has been observed in films in excess of ~250 nm thick.¹⁶ This epitaxial breakdown and loss of the mixed-phase structure, in turn, impose strict limits on the magnitudes of electromechanical response that can be obtained in this material. In this letter, we explore chemical-alloying routes to further stabilize and extend the stability of the sought-after

mixed-phase structures. Using epitaxial thin-film growth, and detailed chemical, structural, and scanning-probe studies, we report on lattice engineering via Pb-alloying as a route to manipulate the structure and strain that stabilizes the highly distorted, tetragonal-like phase and mixed-phase structure to a thickness of greater than 500 nm.

Epitaxial Bi_{1-x}Pb_xFeO₃ (*x* = 0, 0.01, and 0.03) thin films between 20 and 600 nm were grown via pulsed-laser deposition on LaAlO₃ (001) substrates from (Bi_{1-x}Pb_x)_{1.1}FeO_x ceramic targets. Growth was carried out at 700 °C, at an oxygen pressure of 100 mTorr, and at a laser fluence and repetition rate of 1.45 J/cm³ and 10 Hz, respectively. Following growth the films were cooled at an oxygen pressure of 760 Torr. Detailed chemical and structural information, including the extent of Pb-incorporation, overall cation stoichiometry, lattice parameter variation, and the evolution of structural distortions, was obtained using high-resolution x-ray diffraction and reciprocal space mapping (RSM) (X'Pert MRD Pro equipped with a PIXcel detector, Panalytical), x-ray photoelectron spectroscopy (XPS, Kratos Axis XPS, monochromatic Al x-ray source with charge neutralization during collection via electron beam bombardment), and Rutherford backscattering spectrometry (RBS). The topography of the films was studied with atomic force microscopy (AFM), and piezoelectric switching studies were completed using piezoresponse force microscopy (PFM) (Cypher, Asylum Research).

Following growth, the stoichiometry of these films was probed via XPS and RBS. Due to the similar masses of Pb and Bi, RBS alone was not sufficient to accurately probe the cation chemistry of these samples. Calibrated XPS studies revealed stoichiometry transfer of species to the target, but the combination of high growth temperature, the high vapor pressure and, in turn, volatility of Pb, and the re-evaporation of Pb from the films as a self-compensation mechanism leads to considerable Pb-loss. Growth from (Bi_{1-x}Pb_x)_{1.1}FeO_x targets with *x* = 0, 0.25, and 0.50 resulted in final films with [Pb]/[Bi + Pb] fractions of 0%, 1%, and 3%, respectively. The overall chemical composition of the films, in particular the [Bi + Pb]:[Fe] ratio was then probed via RBS. Films grown from all target compositions showed a 1:1 [Bi + Pb]:[Fe] ratio.

^{a)}Electronic mail: lwmartin@illinois.edu.

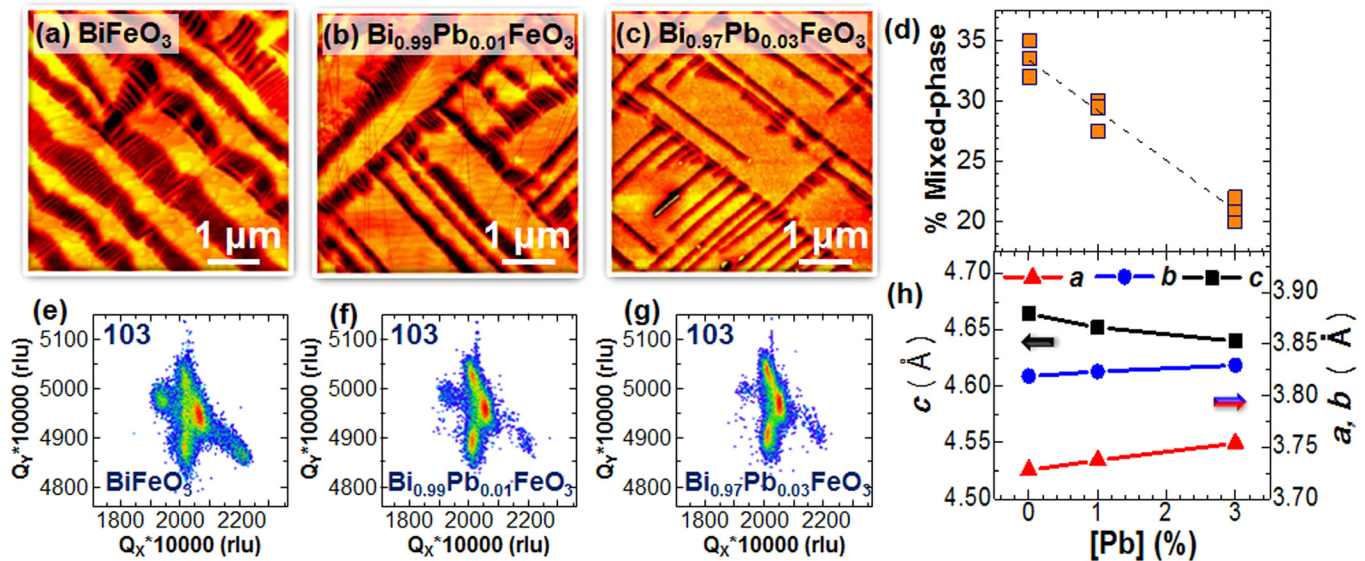


FIG. 1. (Color online) Atomic force microscopy images of 100 nm thick (a) BiFeO₃, (b) Bi_{0.99}Pb_{0.01}FeO₃, and (c) Bi_{0.97}Pb_{0.03}FeO₃ thin films on LaAlO₃ (001) substrates. (d) Evolution of the areal percentage of the mixed-phase regions on these samples as a function of Pb-content. (e)–(g) are reciprocal space maps of the 103-diffraction condition for BiFeO₃, Bi_{0.99}Pb_{0.01}FeO₃, and Bi_{0.97}Pb_{0.03}FeO₃, respectively. (h) In-plane (*a* and *b*) and out-of-plane (*c*) lattice parameters of the M_{II}-phase as a function of Pb-content as determined from the reciprocal space maps.

Structural studies were also completed. Following the nomenclature laid out in recent studies,¹¹ the various phases present in these highly strained films are expected to be the rhombohedral parent phase (R-phase, $c = 3.96 \text{ \AA}$), the highly distorted intermediate monoclinic phase (M_I-phase, $c = 4.17 \text{ \AA}$, tilted $\sim 2.8^\circ$ from the substrate normal), the highly distorted tetragonal-like phase (M_{II}-phase, $c = 4.67 \text{ \AA}$), and a tilted version of the M_{II}-phase (M_{II,tilt}-phase, $c = 4.67 \text{ \AA}$, tilted $\sim 1.6^\circ$ from the substrate normal). Previous studies have shown that the mixed-phase regions of these samples are made up of an intimate mixture of the M_I- and M_{II,tilt}-phases. As evidenced by AFM images of 100 nm thick films of Bi_{1-x}Pb_xFeO₃ ($x = 0, 0.01$, and 0.03) [Figs. 1(a)–1(c), respectively], the surface areal fraction of the mixed-phase regions (stripe-like features) is observed to scale inversely with the Pb-content [Fig. 1(d)]. Upon introducing only 3% Pb into the system, the areal fraction of the mixed-phase regions is observed to decrease by $\sim 12\%$ from that of the BiFeO₃ film.

In order to better understand this effect, we have undertaken a series of high-resolution RSM studies of a number of diffraction peaks to develop a complete picture of the structural changes induced by the Pb-alloying. RSMs of the 103-diffraction peaks [Figs. 1(e)–1(g)] for the M_{II}-phase of the 100 nm thick Bi_{1-x}Pb_xFeO₃ ($x = 0, 0.01$, and 0.03) films reveal a splitting of the peak into three-peaks. These results are consistent with prior studies of this phase and confirm that the M_{II}-phase is monoclinically distorted, with a small tilt along the $\langle 100 \rangle$ in-plane directions.^{9,11,17–19} Furthermore, we note that the side-lobes on either side of the main diffraction peak in Q_x-space are observed to greatly decrease in intensity with increasing Pb-content. This corresponds to a systematic reduction in the fraction of the M_{II,tilt}-phase observed in these films and is consistent with the AFM analysis and with an overall decrease in the fraction of the mixed-phase regime with increasing Pb-content. From these (and other RSM studies, not shown), we can summarize the effect of Pb-alloying on the unit cell of the M_{II}-phase

[Fig. 1(h)]. Overall, the addition of Pb to the BiFeO₃ structure results in an increase of the *a*- and *b*- and a decrease of the *c*-lattice parameter of the material. Such a change in the structure could be the consequence of both the larger ionic radius of Pb²⁺ (assuming 12-fold coordination, 149 pm compared to 138 pm for Bi³⁺) and/or the formation of oxygen vacancies that could accompany the introduction of the Pb²⁺. Key to the enhanced stabilization of the M_{II}-phase is the fact that the Pb-alloying seems to predominantly manifest itself in the form of an increase in the in-plane lattice parameters. The *a*-lattice parameter, for instance, is 3.74 Å, 3.75 Å, and 3.76 Å for the Bi_{1-x}Pb_xFeO₃ films for $x = 0, 0.01$, and 0.03 , respectively. Thus, the Pb-alloying reduces the lattice mismatch between the M_{II}-phase and the LaAlO₃ substrate ($a = 3.79 \text{ \AA}$), further stabilizing the M_{II}-phase, allowing thicker films to be produced prior to relaxation and promoting thicker films with the sought after mixed-phase structures. We note that among the common Bi-site dopants studied for BiFeO₃, only Pb²⁺ and Ba²⁺ (ionic radius of 161 pm, 12-fold coordination) should provide the impetus to further stabilize the tetragonal-like phase of BiFeO₃. This is consistent with the work of Christen *et al.* who observed that Ba-alloying upwards of 8% resulted in a decrease of the monoclinic distortion in the M_{II}-phase and a change in the lattice parameters.⁹

We have also investigated the effect of Pb-alloying on the electromechanical properties of the mixed-phase films using PFM-based local switching studies. We reiterate that large surface strains of 4%-5% are obtained upon electric-field switching of mixed-phase BiFeO₃ samples. Our studies have revealed that the key parameter at play in allowing for the large electromechanical responses is the relative ratio of the various phases in the mixed-phase structures. Since the Pb-alloying alters the areal fraction of the mixed-phase regions significantly, it is important to normalize data appropriately—here we use the areal fraction of the mixed-phase regions as a means of normalization. Thus, we report the

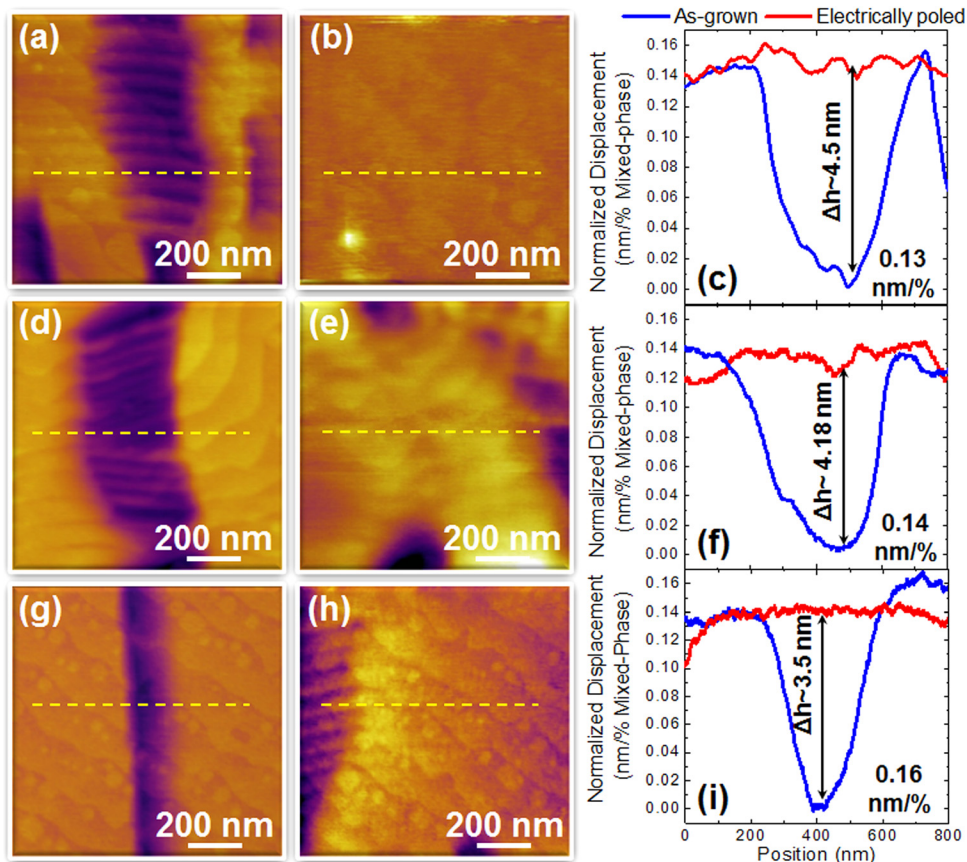


FIG. 2. (Color online) Atomic force microscopy images and corresponding line traces (right) at the dashed line for as-grown (left) and electrically poled (center) 100 nm thick films of (a)–(c) BiFeO_3 , (d)–(f) $\text{Bi}_{0.99}\text{Pb}_{0.01}\text{FeO}_3$, and (g)–(i) $\text{Bi}_{0.97}\text{Pb}_{0.03}\text{FeO}_3$. Note that the height scales in (c), (f), and (i) are normalized to the fraction of mixed-phase regions on these samples for direct comparison.

response both in total magnitude and in nanometers per areal percent of mixed-phase. We have completed local poling on 100 nm $\text{Bi}_{1-x}\text{Pb}_x\text{FeO}_3/\text{LaAlO}_3$ (001) films with $x = 0, 0.01, 0.03$ [Fig. 2]. Consistent with prior results, we observe reversible electromechanical deformations of 4%-5% for BiFeO_3 thin films as we transition from the as-grown [Fig. 2(a)] to the electrically poled state [Fig. 2(b)]. Line traces across the electrically poled region are provided in Fig. 2(c). Similar results are obtained for the $\text{Bi}_{0.99}\text{Pb}_{0.01}\text{FeO}_3$ thin films where we can likewise electrically transform the mixed-phase regions [Fig. 2(d)] to a region of pure M_{II} -phase [Fig. 2(e)] resulting in a net surface displacement [Fig. 2(f)]. We note that the absolute magnitude of the response is diminished slightly, but the response normalized to the total fraction of the mixed-phase is the same if not slightly

enhanced as compared to the BiFeO_3 sample. This same trend is further observed in the $\text{Bi}_{0.97}\text{Pb}_{0.03}\text{FeO}_3$ films [Figs. 2(g)–2(i)]. We observe that the surface strain per unit areal fraction of the mixed-phase region increases from 0.13 nm/% for BiFeO_3 films to 0.16 nm/% for $\text{Pb}_{0.97}\text{Bi}_{0.03}\text{FeO}_3$ films. This is an indication that thicker films of Pb-alloyed BiFeO_3 with similar surface fractions of mixed phase regions will yield a higher net surface displacement in electric-field-induced switching experiments and comparable, if not improved, overall displacement.

To investigate this idea, we studied thick films (300–500 nm) of $\text{Bi}_{0.99}\text{Pb}_{0.01}\text{FeO}_3$ and $\text{Bi}_{0.97}\text{Pb}_{0.03}\text{FeO}_3$ to probe the evolution of phase stability. Fig. 3(a) shows a 10×10 micron scan of a 500 nm $\text{Bi}_{0.99}\text{Pb}_{0.01}\text{FeO}_3/\text{LaAlO}_3$ (001) sample that reveals the presence of the commonly observed mixed-phase

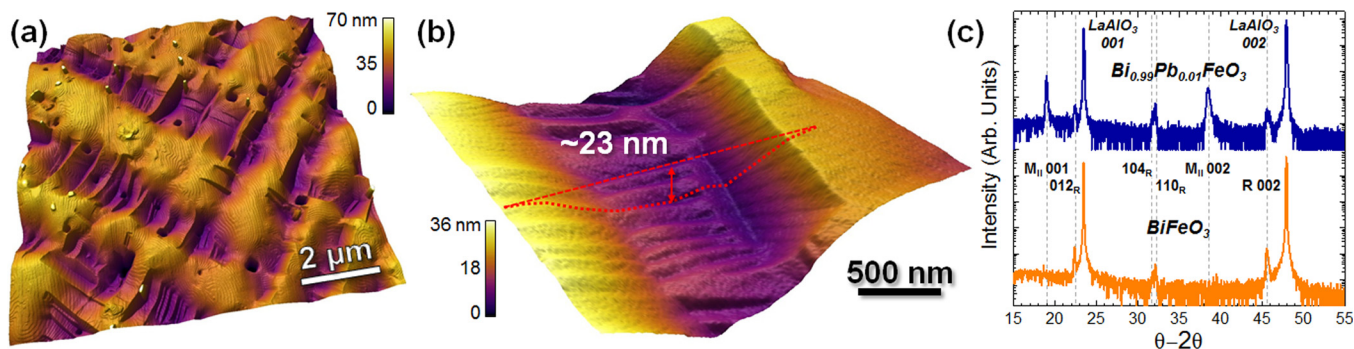


FIG. 3. (Color online) (a) Large scale and (b) zoom-in atomic force microscopy image of a 500 nm thick $\text{Bi}_{0.99}\text{Pb}_{0.01}\text{FeO}_3/\text{LaAlO}_3$ (001) thin film revealing the ability to stabilize the mixed-phase structures necessary for large electromechanical response into thick films. Line-trace across the mixed phase region reveals a surface depression of ~ 23 nm and the capacity for large electromechanical responses. (c) X-ray diffraction results from a (orange data) 300 nm BiFeO_3 film showing complete breakdown and a 500 nm $\text{Bi}_{0.99}\text{Pb}_{0.01}\text{FeO}_3$ film showing the presence of the M_{II} -phase.

regions required for the large electromechanical response. Upon closer inspection [Fig. 3(b)], however, it is evident that these mixed-phase regions possess dramatically increased surface depressions compared to other samples studied. Line traces across a mixed-phase region on this 500 nm thick film reveal surface depressions of ~ 23 nm. This implies that significantly enhanced surface height changes can be observed in these films. To date, we have observed the ability to reversible switch films upwards of 300–350 nm thick (resulting in electromechanical responses as large as 12–14 nm) but have been limited by the lack of a bottom-electrode to enable switching of films in excess of 400–450 nm. Nonetheless, x-ray diffraction studies reveal that 350 nm thick BiFeO₃ thin films possess no evidence of the M_{II}-phase and the mixed-phase structures, while 500 nm thick Bi_{0.99}Pb_{0.1}FeO₃ thin films possess a large fraction of the M_{II}- and mixed-phase structures [Fig. 3(c)]. Overall, Pb-alloying, even in very small amounts, can exact a strong impact on the structure of these materials and helps to stabilize the structures and could enhance overall material performance.

These results have added to our understanding about these complex and technologically exciting phase boundaries in highly strained BiFeO₃ thin films. We have identified that strain engineering via suitable chemical-alloying can delay the onset of epitaxial breakdown in these films and stabilize the necessary nanostructure to assure strong electromechanical responses. By alloying the BiFeO₃ with Pb (1%–3%), we have stabilized the mixed-phase structures to film thicknesses in excess of 500 nm and have demonstrated surface height depressions greater than 20 nm. These observations provide insight into the nature of the phases of BiFeO₃ and their stability and routes to further utilize these materials.

The authors would like to acknowledge the help and scientific insights of Rick Haasch and Doug Jeffers at the Center for Microanalysis of Materials at UIUC. The work at UIUC was supported by the Army Research Office under grant W911NF-10-1-0482 and by Samsung Electronics Co., Ltd. under grant 919 Samsung 2010-06795. Experiments at

UIUC were carried out in part in the Frederick Seitz Materials Research Laboratory Central Facilities, which are partially supported by the U.S. Department of Energy under grants DE-FG02-07ER46453 and DE-FG02-07ER46471.

- ¹W. Eerenstein, N. D. Mathur, and J. F. Scott, *Nature* **442**, 759 (2006).
- ²L. W. Martin, Y.-H. Chu, and R. Ramesh, *Mater. Sci. Eng. R* **68**, 89 (2010).
- ³J. Wang, J. B. Neaton, H. Zheng, V. Nagarajan, S. B. Ogale, B. Liu, D. Viehland, V. Vaithyanathan, D. G. Schlom, U. V. Waghmare *et al.*, *Science* **299**, 1719 (2003).
- ⁴D. Lebeugle, D. Colson, A. Forget, M. Viret, *Appl. Phys. Lett.* **91**, 022907 (2007).
- ⁵C. Ederer and N. A. Spaldin, *Phys. Rev. Lett.* **95**, 257601 (2005).
- ⁶D. Ricinschi, K.-Y. Yun, and M. Okuyama, *J. Phys. Condens. Matter* **18**, L97 (2006).
- ⁷H. Béa, B. Dupé, S. Fusil, R. Mattana, E. Jacquet, B. Warot-Fonrose, F. Wilhelm, A. Rogalev, S. Petit, V. Cros *et al.*, *Phys. Rev. Lett.* **102**, 217603 (2009).
- ⁸R. J. Zeches, M. D. Rossell, J. X. Zhang, A. J. Hatt, Q. He, C.-H. Yang, A. Kumar, C. H. Wang, A. Melville, C. Adamo *et al.*, *Science* **326**, 977 (2009).
- ⁹H. M. Christen, J. H. Nam, H. S. Kim, A. J. Hatt, and N. A. Spaldin, *Phys. Rev. B* **83**, 144107 (2011).
- ¹⁰J. X. Zhang, B. Xiang, Q. He, J. Seidel, R. J. Zeches, P. Yu, S. Y. Yang, C. H. Wang, Y.-H. Chu, L. W. Martin *et al.*, *Nat. Nanotechnol.* **6**, 98 (2011).
- ¹¹A. R. Damodaran, C.-W. Liang, Q. He, C.-Y. Peng, L. Chang, Y.-H. Chu, and L. W. Martin, *Adv. Mater.* **23**, 3170 (2011).
- ¹²F. Zavaliche, S. Y. Yang, T. Zhao, Y. H. Chu, M. P. Cruz, C. B. Eom, and R. Ramesh, *Phase Transitions* **79**, 991 (2006).
- ¹³R. K. Vasudevan, Y. Liu, J. Li, W.-I. Liang, A. Kumar, S. Jesse, Y.-C. Chen, Y.-H. Chu, V. Nagarajan, and S. V. Kalinin, *Nano Lett.* **11**, 3346 (2011).
- ¹⁴H. J. Mamin, R. P. Ried, B. D. Terris, and D. Rugar, *Proc. IEEE* **87**, 1014 (1999).
- ¹⁵*Nanoscale Phenomena in Ferroelectric Thin Films*, edited by S. Hong (Kluwer Academic Boston, MA, 2004).
- ¹⁶A. R. Damodaran, S. Lee, J. Karthik, S. MacLaren, and L. W. Martin, *Phys. Rev. B* **85**, 024113 (2012).
- ¹⁷B. Dupé, I. C. Infante, G. Geneste, P.-E. Janolin, M. Bibes, A. Barthélémy, S. Lisenkov, L. Bellaiche, S. Ravy, and B. Dkhil, *Phys. Rev. B* **81**, 144128 (2010).
- ¹⁸D. Mazumdar, V. Shelke, M. Iliev, S. Jesse, A. Kumar, S. V. Kalinin, A. P. Baddorf, and A. Gupta, *Nano Lett.* **10**, 2555 (2010).
- ¹⁹Z. Chen, Z. Luo, C. Huang, Y. Qi, P. Yang, L. You, C. Hu, T. Wu, J. Wang, C. Gao *et al.*, *Adv. Funct. Mater.* **21**, 133 (2011).